We are IntechOpen,
the world's leading publisher of Open Access books
Built by scientists, for scientists

6,900
Open access books available

186,000
International authors and editors

200M
Downloads

Our authors are among the

154
Countries delivered to

TOP 1%
most cited scientists

12.2%
Contributors from top 500 universities

CLARIVATE ANALYTICS
BOOK CITATION INDEX
INDEXED

WEB OF SCIENCE™

Selection of our books indexed in the Book Citation Index
in Web of Science™ Core Collection (BKCI)

Interested in publishing with us?
Contact book.department@intechopen.com

Numbers displayed above are based on latest data collected.
For more information visit www.intechopen.com

Color Image Watermarking Based on Radon Transform and Jordan Decomposition

Pranab Kumar Dhar, Rakib Hasan and
Tetsuya Shimamura

Abstract

Digital watermarking has been widely used for ownership identification and copyright protection. In this chapter, a color image watermarking method based on Radon transform (RT) and Jordan decomposition (JD) is proposed. Initially, the host color image is converted into L*a*b* color space. Then, the b* channel is selected and it is divided into 16×16 non-overlapping blocks. RT is applied to each of these blocks. JD is applied to the selected RT coefficients of each block represented in m × n matrix. Watermark data is embedded in the coefficients of the similarity transform matrix obtained from JD using a new quantization equation. Experimental results indicate that the proposed method is highly robust against various attacks such as noise addition, cropping, filtering, blurring, rotation, JPEG compression etc. In addition, it provides high quality watermarked images. Moreover, it shows superior performance than the state-of-the-art methods reported recently in terms of imperceptibility and robustness.

Keywords: imperceptibility, quantization, Jordan decomposition, radon transform, robustness

1. Introduction

Internet is the fastest growing medium of transferring data to any place in the world. The creation and distribution of digital media content is increasing day by day. With the recent proliferation of the internet, the threat of privacy and copyright of digital content has become an important issue. Digital watermarking is the most secured way to protect copyright protection and authentication.

Various types of image watermarking methods have been proposed in past decades. Two types of watermarking techniques are used according to domain [1]. In the spatial domain techniques, the watermark is embedded in the pixel values of an image. Least significant bit (LSB) watermarking is the most common spatial domain embedding technique. It is not an effective way to embed watermark because the watermark can be easily removed or modified. In transform domain techniques, the watermark is embedded into the coefficients of the transformed domain. Discrete wavelet transform (DWT), discrete cosine transform (DCT) and discrete Fourier transform (DFT) are the most common transformations that are utilized in transform domain techniques. A novel blind watermarking algorithm in DCT domain using the correlation between two DCT coefficients of adjacent blocks in the same position is proposed by Das et al. [2]. Sadreazami et al. [3] used a blind watermarking scheme in the wavelet-based contourlet domain. For embedding, they used an even-odd quantization technique. A multipurpose image watermarking scheme is proposed by Ansari and Pant [4] in order to provide tamper localization, self-recovery and ownership verification of the host image. Choudhary and Parmar [5] introduced a robust image watermarking technique using two-level DWT. However, the peak signal-to-noise-ratio (PSNR) is quite low and they did not assess the robustness against malicious attack. Recently, singular value decomposition (SVD) has been widely used in image watermarking. Siddiqui and Kaur [6] proposed a hybrid method based on DWT and SVD. The robustness of this method is good but the PSNR of the watermarked image is little low. Another DWT and SVD-based image watermarking method is presented by Srilakshmi and Himabindu [7]. The PSNR of this method is good but the robustness against attacks is low. Savakar and Ghuli [8] proposed multiple methods such as single level DWT, DFT, SVD to embed watermark. The PSNR of this method is quite low.

Very few papers utilized Radon transform (RT) in watermarking. Siddik and Elbasi [9] introduced a watermarking technique using RT. Rastegar et al. [10] proposed a hybrid watermarking algorithm based on RT and SVD. They also used 2D-DWT in the RT domain. The PSNR of this method is good but robustness of this method against malicious attacks is low. To overcome the limitations, in this chapter, we propose an image watermarking method based on RT and Jordan decomposition (JD). To the best of our knowledge, this is the first image watermarking method based RT and JD. The main features of the proposed method include (i) it utilizes the RT, JD and quantization jointly, (ii) the watermark bits are embedded into the similarity transform matrix of the RT coefficients obtained from b channel of the original host image using a new quantization equation, (iii) it provides high robustness against various attacks as well as good quality watermarked images, and (iv) it achieves a good trade-off between imperceptibility and robustness (v) it shows superior performance than the state-of-the-art methods in terms of imperceptibility and robustness. The peak signal-to-noise ratio (PSNR) and structural similarity (SSIM) of the proposed method range from 47.4997 to 51.8848 and 0.9989 to 0.9998, respectively. On the other hand, PSNR and SSIM of the recent methods [4, 11] range from 29.5667 to 34.4495 and 0.9507 to 0.9907, respectively. The normalized correlation (NC) of the proposed method for various attacks ranges from 0.9939 to 1, in contrast to the recent methods whose NC range from 0.0020 to 0.9996.

The rest of the chapter is organized as follows. Section 2 provides a background information including RT and JD. The proposed watermarking method is introduced in Section 3. Section 4

compares the performance of the proposed method with some recent methods in terms of imperceptibility and robustness. Finally, Section 5 concludes this chapter.

2. Background information

2.1. Radon transform (RT)

Johann Radon invented RT in 1917 also provided the formula for the inverse transform (**Figure 1**). The Radon transform is an integral transform that takes a function f defined on the plane to a function R_f defined on the (two-dimensional) space of lines in the plane. Its value at a particular line is equal to the line integral of the function over that line [12].

The Radon transform can be expressed as follows:

$$Rf(\alpha, s) = \int_{-\infty}^{\infty} f(x(z), y(z))dz$$
$$= \int_{-\infty}^{\infty} f((z \sin \alpha + s \cos \alpha), (-z \cos \alpha + s \sin \alpha))dz$$

(1)

After applying inverse radon transform, we can reconstruct the original image quite well. RT has been widely used in various applications of image processing. RT has excellent feature to
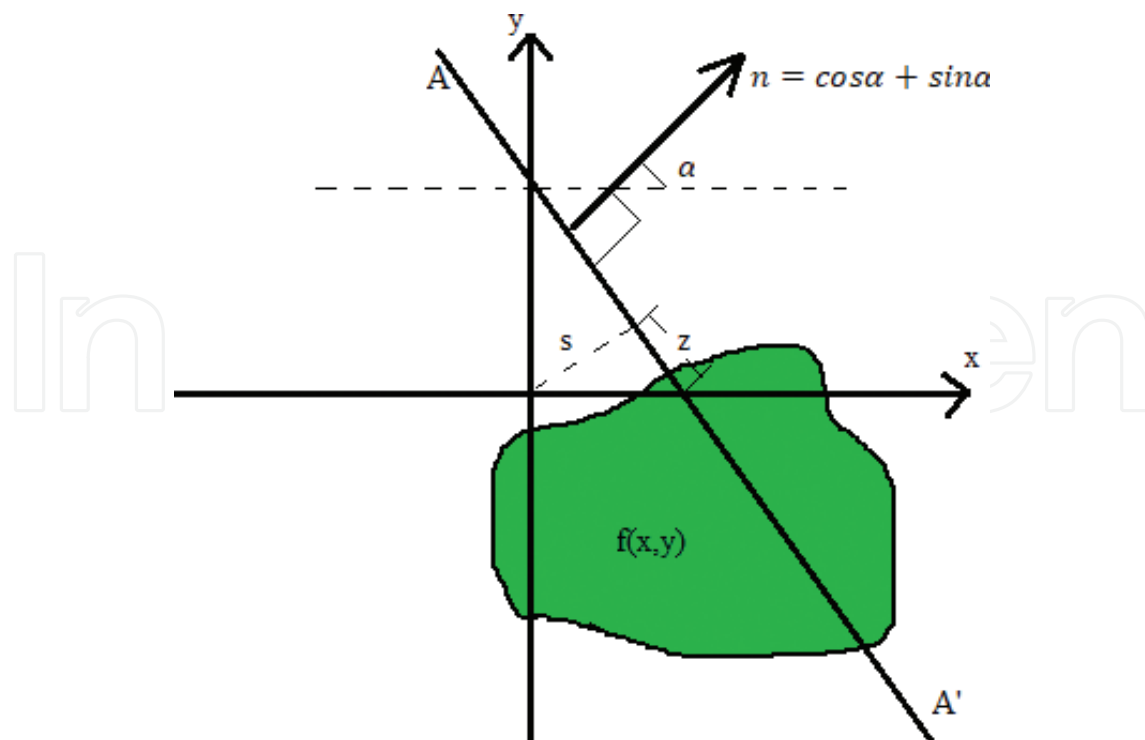

Figure 1. Radon transform that maps f on the (x,y) domain to the (α, s) domain.

transform the information from two-dimensional image into a string of one-dimensional projections which is computationally faster. It has the following advantages:

i.   It has the ability to detect line width and has good robustness for noisy images.

ii. If the image scaled as angle θ, RT is also changed according to same size

$$I\big(x\cos\phi - y\sin\phi + y\cos\phi\big) \leftrightarrow R\big(x, \theta + \phi\big).$$

iii. If image resized as p, RT is also change with same size

$$I(px, py) \leftrightarrow \frac{1}{p}R(pX, \theta)$$

RT produces a big matrix by computing projections of an image along specified direction. For this reason, there is very little effect of embedding watermark in RT domain, which provides high quality watermarked images as well as good robustness against various attacks.

2.2. Jordan decomposition

Jordan decomposition (also known as Jordan normal form or Jordan canonical form) results from the conversion of a matrix into its diagonal form by a similarity transformation [13]. The Jordan matrix decomposition of a square matrix A can be represented by:

$$A = VJV^{-1} \tag{2}$$

Here, the Jordan normal form J is the diagonal matrix of eigenvalues and the similarity transform matrix V contains the generalized eigenvectors as columns. The use of similarity transform aims at reducing the complexity of the problem of evaluating the eigenvalues of a matrix. Indeed, if a given matrix could be transformed into a similar matrix in diagonal form, the computation of the eigenvalues would be easy. Moreover, the slight variations of eigenvalues in embedding watermark have little effect on the quality of the watermarked image. For this reason, it provides high quality watermarked images as well as good robustness against various attacks.

3. Proposed watermarking method

Let $I = \{i(u, v), 1 \le u \le M, 1 \le v \le M\}$ be the host image and $W = \{w(k, l), 1 \le k \le N, 1 \le j \le N\}$ be a binary watermark image to be embedded into the host image.

The proposed watermarking method is described in this section which can be divided into two parts (i) watermark embedding process and (ii) watermark extraction process.

3.1. Watermark embedding process

The watermark embedding process is shown in **Figure 2** and it can be stated as follows:

1. The original host image *I* is converted into L*a*b* color space denoted by I_L, I_a, and I_b.

2. The I_b channel is selected and this channel is divided into $n \times n$ non-overlapping blocks denoted by B_a with a border size of 1×1.

3. RT is applied on each block B_a of the color space I_b. After applying RT, transformed matrix R_b is obtained.

4. JD is applied to a part of the matrix R_b of size $p \times p$ denoted by R_{bs}. This is because computational cost of JD is quite high and it takes long time to perform on a big matrix. The JD can be represented as follows:

$$R_{bs} = V_C J_C V_C^{-1} \tag{3}$$

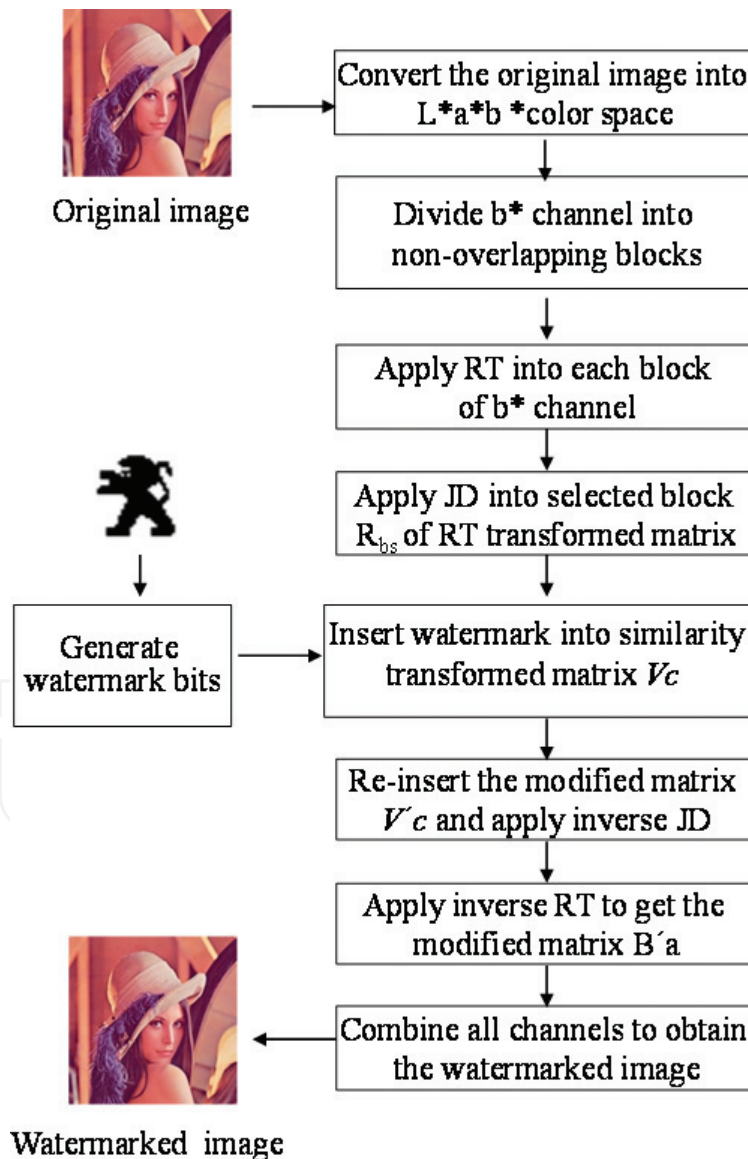Here, *Jc* is the Jordan normal form and *Vc* is the similarity transform matrix.

Figure 2. Watermark embedding process.

5. In order to guarantee the robustness and imperceptibility, the proposed algorithm embeds watermark bit into all coefficients of similarity transform matrix V_C using a new quantization function. This ensures that the watermark is located at the most significant perceptual components of the image. Watermark data is embedded by using the following equation:

$$V_C'(i,j) = \begin{cases} V_C(i,j) + \dfrac{B \bmod(q)}{V_{\max} \times \Delta} + (V_{\max} \times \Delta) \, if \, W(k,l) = 1 \\ V_C(i,j) - \Delta \, if \, W(k,l) = 0 \end{cases} \tag{4}$$

where, B is the current block number, q is an integer, Δ is an integer, V_{max} is the maximum value of matrix V_C.

6. Reinsert each modified coefficient $V'_c(i, j)$ into matrix V'_c and inverse JD is applied to obtain the modified matrix R'_{bs}.

7. Reinsert each modified matrix R'_{bs} into R_b to obtain modified matrix R'_b.

8. Inverse RT is applied to each modified matrix R'_b to get the modified block B'_a.

9. All modified blocks are combined to obtain the modified color space $I_{b'}$.

10. Finally, all the channels I_{L^*}, I_{a^*}, and I'_{b^*} are combined to get the watermarked image I'.

3.2. Watermark extraction process

In watermark extraction process, both the original host image I and attacked watermarked image I^* are used, which is shown in **Figure 3** and can be described as follows:

1. The original host image I and attacked watermarked image I^* are converted into L*a*b* color space denoted by I_L, I_a, I_b and I^*_L, I^*_a, I^*_b, respectively.

2. The I_b and I^*_b channel of I and I^* are selected and divided into $n \times n$ non-overlapping blocks denoted by B_a and B^*_a, respectively with a border size of 1×1.

3. RT is applied on each block B_a and B^*_a of the color space I_b and I'_b, respectively. After applying RT, transformed matrix R_b and R^*_b are obtained.

4. JD is applied to a part of the matrix R_b and R^*_b of size $p \times p$ denoted by R_{bs} and R^*_{bs} to obtain the two Jordan matrices J_C, J_C^* and two similarity transform matrices V_C, V_C^*, respectively.

5. To extract the watermark bits, the transform matrices V_C and V_C^* are compared. If the selected coefficients extracted from V_C^* is less than or equal to that of V_C, then the extracted watermark bit will be '0'. Otherwise, the extracted watermark bit will be '1'. This can be expressed as follows:

$$W^*(k,l) = \begin{cases} 0 \; if \; V_C^*(k,l) \leq V_C(k,l) \\ 1 \; otherwise \end{cases} \tag{5}$$

where $V_C(k,l)$ and $V_C^*(k,l)$ are the extracted value from the original and attacked watermarked image and $W^*(k,l)$ is the extracted watermark bit.

6. After extracting all the watermark bits, the binary watermark image W^* is obtained.
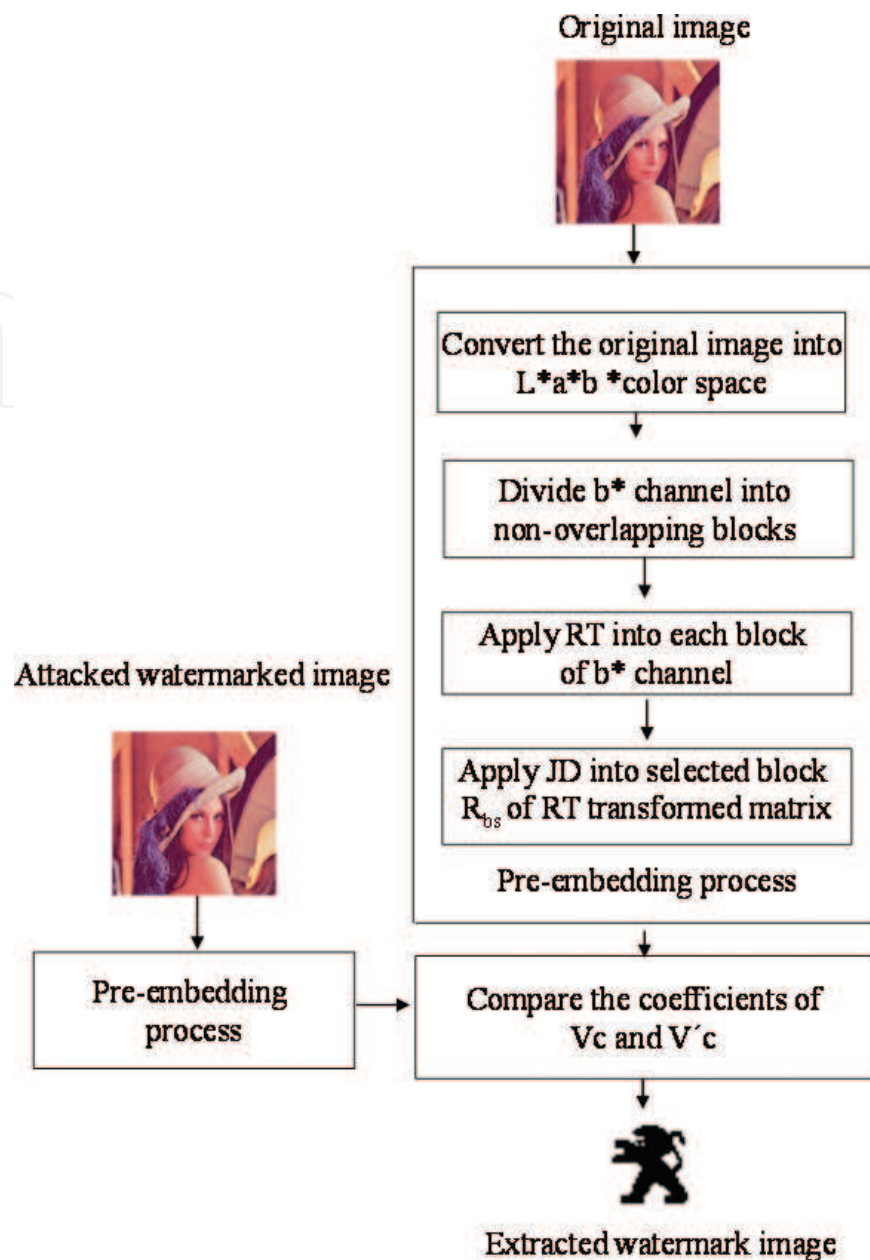
Figure 3. Watermark extraction process.

4. Experimental results

In this section, we have evaluated the performance of our proposed method in terms of imperceptibility and robustness. We carried out several experiments and also compared with some recent methods. In this study, we used four color JPEG images of size 256×256 from the USC-SIPI image database [14] shown in **Figure 4**. The binary watermark image of size 32×32 is used in our experiment taken from the Free Stencil Gallery [15] shown in **Figure 5**. In this study, for simplicity the selected value for n and p are 16 and 2, respectively. Computational cost of JD is quite high and it takes long time to perform JD on a big matrix. For this reason, we have selected a small value for p.
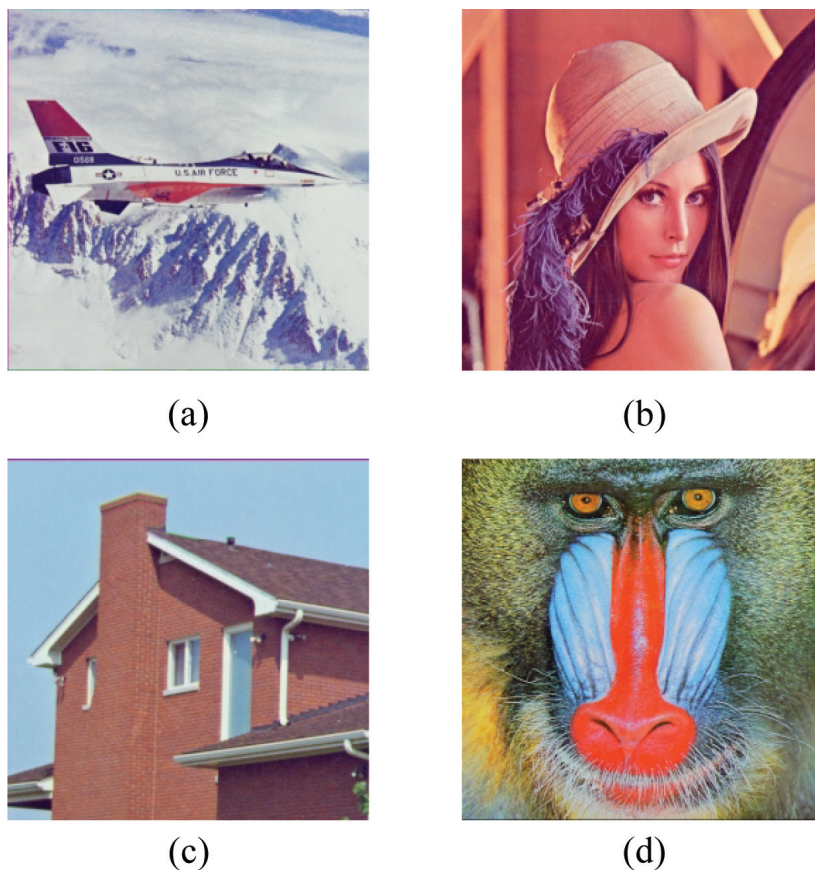
Figure 4. Host images used in our experiment (a) airplane, (b) Lena, (c) house, and (d) baboon.

Figure 5. Watermark image use in our experiment.

4.1. Imperceptibility

To test the imperceptibility of the proposed method, we have calculated peak signal-to-noise ratio (PSNR) and structural similarity index measurement (SSIM) watermarked images.

PSNR is calculated using the following equation:

$$PSNR = 10 \log_{10} \left(\frac{255^2}{\frac{1}{MM} \sum\limits_{k=1}^{M} \sum\limits_{l=1}^{M} \left(A - A'\right)^2} \right) \tag{6}$$

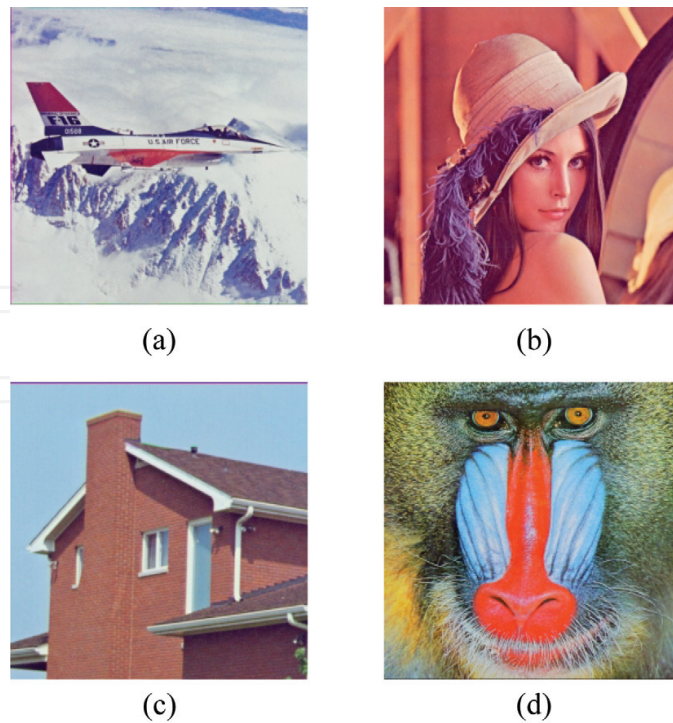The watermarked images are shown in **Figure 6**.

Figure 6. Watermarked images obtained in this experiment (a) airplane, (b) Lena, (c) house, and (d) baboon.

SSIM is an efficient method for measuring the similarity between two images and it can be expressed as:

$$SSIM(A, A') = \frac{(2\mu_I\mu_{I'} + c_1)(2\sigma_{II'} + c_2)}{(\mu_I^2 + \mu_{I'}^2 + c_1)(\sigma_I^2 + \sigma_{I'}^2 + c_2)} \tag{7}$$

Here, μ_I, σ_I, $\mu_{I'}$, $\sigma_{I'}$, and $\sigma_{II'}$ indicate the mean of I, variance of I, mean of I', variance of I', covariance of I and I', respectively. c_1, and c_2 are the two variables used in Eq. (7).

Table 1 shows the PSNR comparison between the proposed scheme and two recent methods. Ansari and Pant [4] used DWT-SVD domain to embed watermark. This method has an average PSNR value of 34.4356. Al-Afandy et al. [11] used discrete stationary wavelet transform (DSWT) in the DCT domain to embed watermark. This method has an average PSNR value of 33.1474 and ranges from 29 to 36. This is in contrast to the proposed method whose PSNR values ranges from 47.4997 to 51.8848 and the average value is 49.0387.

Table 1 also shows the SSIM comparison between the proposed scheme and two recent methods. The more the SSIM value approaches to 1, the better the image quality is. Our proposed method provides SSIM values close to 1 which is excellent for a watermarked image. Also, the proposed method shows higher SSIM values compared to the recent methods.

Radon transform generates a large matrix from the given image matrix which is convenient for embedding watermark. For this reason, we have used a small portion of transformed matrix for watermark insertion. Hence, there is very little effect on embedding watermark into the host image and we obtained higher PSNR, SSIM values compared to the conventional methods.

Image	Measurement	Ansari and Pant [4]	Al-Afandy et al. [11]	Proposed
Airplane	PSNR	34.4495	33.6072	49.2705
	SSIM	0.9672	0.9507	0.9989
Lena	PSNR	34.4339	34.2382	51.8848
	SSIM	0.9701	0.9907	0.9998
House	PSNR	34.4196	35.1776	47.4997
	SSIM	0.9694	0.9833	0.9995
Baboon	PSNR	34.4393	29.5667	47.4997
	SSIM	0.9889	0.9529	0.9993
Ave range	PSNR	49.0387	33.1474	49.0387
	SSIM	0.9889	0.9529	0.9993

Table 1. Comparison between the proposed scheme and several recent methods in terms of PSNR and SSIM.

4.2. Robustness

To assess the robustness, we have calculated normalized correlation (NC) which computes the difference between original watermark and the extracted watermark. The equation of NC is given below:

$$NC(W, W^*) = \frac{\sum_{k=1}^{N} \sum_{l=1}^{N} w(k,l) \cdot w^*(k,l)}{\sqrt{\sum_{k=1}^{N} \sum_{l=1}^{N} w(k,l) \cdot w(k,l)} \sqrt{\sum_{k=1}^{N} \sum_{l=1}^{N} w^*(k,l) \cdot w^*(k,l)}} \qquad (8)$$

where k and l are the indices of the binary watermark image. The correlation between W and W^* is very high when NC (W, W^*) is close to 1. On the other hand, the correlation between W and W^* is very low when NC (W, W^*) is close to zero.

From **Figure 7**, we observed that NC varies when quantization step size Δ is below 6. NC remains constant at 1 when $\Delta \geq 6$. In this study, the selected value for Δ is 15.
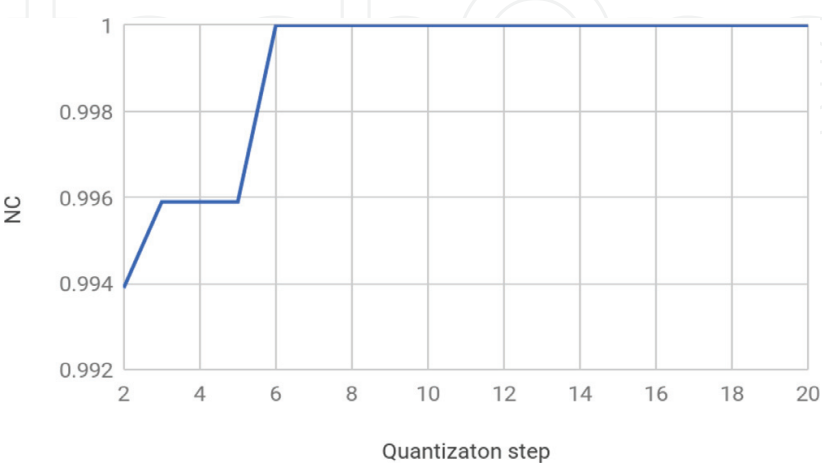

Figure 7. NC vs. quantization step size.

Figure 8. Different types of attacks applied to watermarked image 'Lena' (a) JPEG(30), (b) JPEG(90), (c) JPEG 2000, (d) salt & pepper noise, (e) Gaussian white noise, (f) speckle noise, (g) median filter, (h) wiener filter, (i) crop (25%) (j) rotation 25°, (j) sharpened, and (k) blurred.

Figure 9. Extracted watermark image after applying various attacks on 'Lena' image (a) JPEG(30), (b) JPEG(90), (c) JPEG 2000, (d) salt & pepper noise, (e) Gaussian white noise, (f) speckle noise, (g) median filter, (h) wiener filter, (i) crop (25%), (j) rotation 25°, (j) sharpened, and (k) blurred.
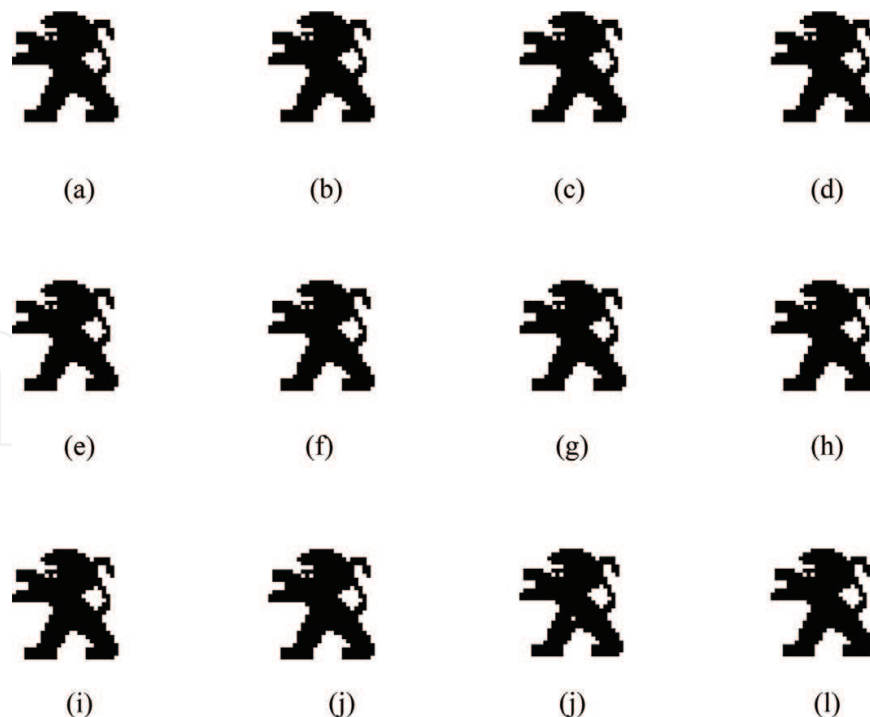
To verify the robustness of our proposed method, we applied different malicious attacks such as noise addition, cropping, rotation, filtering, blurring, sharpening, JPEG compression etc. on the watermarked image. **Figure 8** shows the effects of attacks on the watermarked image 'Lena'. We can also observe the watermark image extracted from the attacked watermarked image in **Figure 9**. From this figures, we observed that our proposed method shows high robustness against various attacks. **Tables 2** and **3** show the NC comparison between the proposed scheme and several recent methods against various attacks. The method proposed by Ansari and Pant [4] show good robustness where NC values range from 0.0020 to 0.9961. But, this method cannot resist against cropping and rotation attack. The method proposed by Al-Afandy et al. [11] proposed method shows good robustness and the NC values of this range

Attack	Images	Proposed	Ansari and Pant [4]	Al-Afandy et al. [11]
JPEG(30)	Airplane	1	0.9689	0.9997
	Lena	1	0.9702	0.9997
	House	0.9980	0.9685	0.9995
	Baboon	1	0.9961	0.9998
JPEG(90)	Airplane	1	0.9956	0.9998
	Lena	1	0.9956	0.9997
	House	0.9980	0.9957	0.9995
	Baboon	1	0.9953	0.9997
JPEG 2000	Airplane	1	0.9955	0.9998
	Lena	1	0.9955	0.9997
	House	0.9980	0.9957	0.9995
	Baboon	1	0.9951	0.9998
Salt and pepper noise	Airplane	0.9980	0.6008	0.9991
	Lena	1	0.5895	0.9973
	House	0.9959	0.6373	0.9992
	Baboon	1	0.6236	0.9984
Gaussian white noise	Airplane	0.9980	0.7293	0.9992
	Lena	1	0.7453	0.9963
	House	0.9959	0.7158	0.9992
	Baboon	1	0.7284	0.9989
Speckle noise	Airplane	1	0.4654	0.9994
	Lena	1	0.6181	0.9991
	House	0.9939	0.5542	0.9996
	Baboon	1	0.6099	0.9993
Median filter	Airplane	1	0.9961	0.9996

Table 2. NC comparison between the proposed scheme and several methods against various noise and JPEG compression attacks.

Attack	Images	Proposed	Ansari and Pant [4]	Al-Afandy et al. [11]
Median filtering	Airplane	1	0.9961	0.9996
	Lena	1	0.9960	0.9996
	House	0.9980	0.9961	0.9994
	Baboon	1	0.9956	0.9993
Wiener filtering	Airplane	0.9980	0.9961	0.9996
	Lena	1	0.9960	0.9996
	House	1	0.9961	0.9994
	Baboon	1	0.9956	0.9995
Cropping 25%	Airplane	1	0.0707	0.9997
	Lena	1	0.0551	0.9996
	House	0.9980	0.0588	0.9994
	Baboon	1	0.0020	0.9996
Rotation 25°	Airplane	1	0.0216	0.9974
	Lena	1	0.0738	0.9981
	House	0.9980	0.0155	0.9983
	Baboon	1	0.0715	0.9990
Sharpening	Airplane	1	0.9748	0.9996
	Lena	0.9980	0.9762	0.9983
	House	0.9959	0.9802	0.9996
	Baboon	1	0.9755	0.9977
Blurring	Airplane	1	0.5738	0.9994
	Lena	1	0.6673	0.9993
	House	0.9980	0.6496	0.9992
	Baboon	1	0.7478	0.9990

Table 3. NC comparison between the proposed scheme and several methods against filtering, cropping, rotation, sharpening, and blurring attacks.

from 0.9977 to 0.9997. Our proposed method shows higher NC values than these method against various attacks. This is because watermark is embedded into the similarity transform matrix of the RT coefficients obtained from b channel of the original host image using a new quantization equation.

5. Conclusions

In this chapter, we have introduced a color image watermarking method based on RT and JD. Simulation results demonstrate that the proposed method is highly robust against different

attacks such as noise addition, cropping, filtering, rotation, blurring, sharpening, and JPEG compression. In addition, it provides high quality watermarked images. Moreover, it outperforms state-of-the-art image watermarking methods in terms of imperceptibility and robustness. These results indicate that the proposed watermarking method can be used for image copyright protection.

Author details

Pranab Kumar Dhar[1]*, Rakib Hasan[1] and Tetsuya Shimamura[2]

*Address all correspondence to: pranabdhar81@gmail.com

1 Department of Computer Science and Engineering, Chittagong University of Engineering and Technology (CUET), Chittagong, Bangladesh

2 Graduate School of Science and Engineering, Saitama University, Saitama, Japan

References

[1] Tyagi S, Singh HV, Agarwal R, Gangwar SK. Digital watermarking techniques for security applications. In: 2016 International Conference on Emerging Trends in Electrical Electronics & Sustainable Energy Systems (ICETEESES); 2016

[2] Das C, Panigrahi S, Sharma VK, Mahapatra K. A novel blind robust image watermarking in DCT domain using inter-block coefficient correlation. AEU - International Journal of Electronics and Communications. 2014;**68**(3):244-253

[3] Sadreazami H, Ahmad MO, Swamy MNS. A robust quantization-based image watermarking scheme in the wavelet-based contourlet domain. In: 2016 IEEE Canadian Conference on Electrical and Computer Engineering (CCECE); 2016

[4] Ansari A, Pant M. Multipurpose image watermarking in the domain of DWT based on SVD and ABC. Pattern Recognition Letters. 2017;**94**:228-236

[5] Choudhary R, Parmar G. A robust image watermarking technique using 2-level discrete wavelet transform (DWT). In: 2016 2nd International Conference on Communication Control and Intelligent Systems (CCIS); 2016

[6] Siddiqui A, Kaur A. A secure and robust image watermarking system using wavelet domain. In: 2017 7th International Conference on Cloud Computing, Data Science & Engineering - Confluence; 2017

[7] Srilakshmi P, Himabindu C. Image watermarking with path based selection using DWT & SVD. In: 2016 IEEE International Conference on Computational Intelligence and Computing Research (ICCIC); 2016

[8]   Savakar DG, Ghuli A. Non-blind digital watermarking with enhanced image embedding capacity using DMeyer wavelet decomposition, SVD, and DFT. Pattern Recognition and Image Analysis. 2017;**27**(3):511-517

[9]   Siddik O, Elbasi E. Information hiding: A new multi watermark algorithm using radon transformation. International Journal of Information and Electronics Engineering. 2015; **5**(6):460-463

[10] Rastegar S, Namazi F, Yaghmaie K, Aliabadian A. Hybrid watermarking algorithm based on singular value decomposition and radon transform. AEU - International Journal of Electronics and Communications. 2011;**65**(7):658-663

[11] Al-Afandy KA, Faragallah OS, El-Rabaie E-S M, El-Samie FEA, Elmhalawy A. A hybrid scheme for robust color image watermarking using DSWT in DCT domain. In: 2016 4th IEEE International Colloquium on Information Science and Technology (CiSt); 2016

[12] Radon Transform. Wikipedia [Online]. Available from: https://en.wikipedia.org/wiki/Radon_transform

[13] Documentation. Jordan Canonical Form - MATLAB & Simulink [Online]. Available from: https://www.mathworks.com/help/symbolic/jordan-canonical-form.html

[14] The USC-SIPI Image Database [Online]. Available from: http://sipi.usc.edu/database/

[15] Peugeot Logo Stencil. Free Stencil Gallery [Online]. Available from: http://www.freestencilgallery.com/peugeot-logo-stencil